Collisional energy loss and the chiral magnetic effect

Jeremy Hansen and Kirill Tuchin

Department of Physics and Astronomy, Iowa State University, Ames, Iowa 50011, USA

Collisional energy loss of a fast particle in a medium is mostly due to the medium polarization by the electromagnetic fields of the particle. A small fraction of energy is carried away by the Cherenkov radiation. In chiral medium there is an additional contribution to the energy loss due to induction of the anomalous current proportional to the magnetic field. It causes the particle to lose energy mostly in the form of the *chiral* Cherenkov radiation. We employ classical electrodynamics, adequate in a wide range of particle energies, to compute the collisional energy loss by a fast particle in a homogenous chiral plasma and apply the results to quark-gluon plasma and a Weyl semimetal. In the latter case photon spectrum is strongly enhanced in the ultraviolet and x-ray regions which makes it amenable to experimental investigation. Our main observation is that while the collisional energy loss in a nonchiral medium is a slow, at most logarithmic, function of energy ε, the chiral Cherenkov radiation is proportional to ε^2 when the recoil is neglected and to ε when it is taken into account.

I. INTRODUCTION

A fast charged particle moving through a medium experiences energy loss due to its interaction with medium particles. The collisional part of the energy loss equals the work done by the induced electromagnetic field on displacing the medium particles. If the particle energy is much larger than the typical ionization energy, then the collisional part of its energy loss depends on the macroscopic medium response to the electromagnetic field. The unique feature of such response in materials containing chiral fermions is the chiral magnetic effect [1–5] which is induction—by the way of the chiral anomaly [6,7]—of anomalous electric current flowing in the magnetic field direction. The work spent by the particle on inducing the anomalous current contributes to its energy loss. The goal of this paper is to calculate this anomalous part of the collisional energy loss.

The classical calculation of the collisional energy loss in the nonchiral medium was first preformed by Fermi [8]. We generalize his calculation to the chiral medium with anomalous response to the magnetic field, utilizing the recently derived expressions for the electromagnetic field [9]. Our main conclusion is that the energy loss in the chiral medium is proportional to the particle energy itself and comes mostly in the form of the chiral Cherenkov radiation—an analog of the Cherenkov radiation that exist only in the chiral medium.

This is in striking contrast with the collisional energy loss in nonchiral medium which is independent of the particle's energy in the ultrarelativistic limit. We also argue that in a wide range of particle energies, quantum corrections due to the recoil effects are small.

The collisional energy loss spectrum is given by Eqs. (10)–(18). It contains the anomalous contribution, mostly due to the chiral Cherenkov radiation, which is clearly seen in Fig. 1 for quark-gluon plasma and in Fig. 2 for a Weyl semimetal. In the latter case the photon spectrum is strongly enhanced in the ultraviolet and x-ray regions which makes it amenable to experimental investigation.

II. ELECTROMAGNETIC FIELDS IN CHIRAL MEDIUM

Electrodynamics of isotropic chiral medium is characterized by the emergence of the anomalous current proportional to the magnetic field viz. $\boldsymbol{j}_A = \sigma_\chi \boldsymbol{B}$, where σ_χ is the chiral conductivity [1,14]. As a result, the field equations for a point charge q moving in the positive z direction with constant velocity v read:

$$\nabla \times \boldsymbol{B} = \partial_t \boldsymbol{D} + \sigma_\chi \boldsymbol{B} + qv\hat{\boldsymbol{z}}\delta(z - vt)\delta(\boldsymbol{b}), \tag{1a}$$

$$\nabla \cdot \boldsymbol{D} = q\delta(z - vt)\delta(\boldsymbol{b}), \tag{1b}$$

$$\nabla \times \boldsymbol{E} = -\partial_t \boldsymbol{B}, \tag{1c}$$

$$\nabla \cdot \boldsymbol{B} = 0, \tag{1d}$$

where $\boldsymbol{b}$ denotes the transverse components of the position vector $\boldsymbol{r}$. The solution to (1) with $\boldsymbol{D}_\omega = \epsilon(\omega)\boldsymbol{E}_\omega$, where $E_z = \frac{1}{2\pi}\int_{-\infty}^{\infty} E_{z\omega}e^{-i\omega t}d\omega$, etc., was derived in Ref. [9] as a
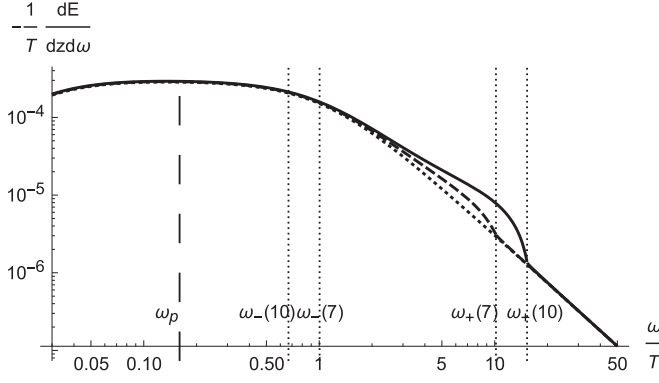
FIG. 1. Electromagnetic part of the collisional energy loss spectrum of a d-quark with $\gamma = 20$ in quark-gluon plasma. Plasma parameters: $\omega_p = 0.16T$, $\Gamma = 1.11T$ [10], $m = T = 250$ MeV. Solid line: $\sigma_\chi = 10$ MeV, dashed line: $\sigma_\chi = 7$ MeV, dotted line: $\sigma_\chi = 0$. $\omega_\pm$ are defined in (13). The QCD contribution has a similar shape and is about 10^3–10^4 times larger in magnitude.

superposition of the helicity states $\lambda = \pm 1$, which are the eigenstates of the curl operator in the Cartesian coordinates:

$$\boldsymbol{B}(\boldsymbol{r}, t) = \int \frac{d^2k_\perp d\omega}{(2\pi)^3} e^{i\boldsymbol{k}\cdot\boldsymbol{r} - i\omega t}$$
$$\times \sum_\lambda \boldsymbol{\epsilon}_{\lambda k} \frac{q\hat{\boldsymbol{z}} \cdot \boldsymbol{\epsilon}_{\lambda\boldsymbol{k}}^* \lambda k}{k_\perp^2 + \omega^2(1/v^2 - \epsilon) - \lambda\sigma_\chi k}, \quad (2a)$$

$$\boldsymbol{E}(\boldsymbol{r}, t) = \int \frac{d^2k_\perp d\omega}{(2\pi)^3} e^{i\boldsymbol{k}\cdot\boldsymbol{r} - i\omega t}$$
$$\times \left[\sum_\lambda \boldsymbol{\epsilon}_{\lambda k} \frac{iq\omega\hat{\boldsymbol{z}} \cdot \boldsymbol{\epsilon}_{\lambda\boldsymbol{k}}^*}{k_\perp^2 + \omega^2(1/v^2 - \epsilon) - \lambda\sigma_\chi k} + \hat{\boldsymbol{k}} \frac{q}{iv k\varepsilon} \right], \quad (2b)$$

where $\boldsymbol{k} = \boldsymbol{k}_\perp + (\omega/v)\hat{\boldsymbol{z}}$ is the wave vector, $k = \sqrt{k_\perp^2 + \omega^2/v^2}$ its length, and $\boldsymbol{\epsilon}_{\lambda k}$ are the circular polarization vectors satisfying the conditions $\boldsymbol{\epsilon}_{\lambda k} \cdot \boldsymbol{\epsilon}_{\mu k}^* = \delta_{\lambda\mu}$, $\boldsymbol{\epsilon}_{\lambda k} \cdot \boldsymbol{k} = 0$
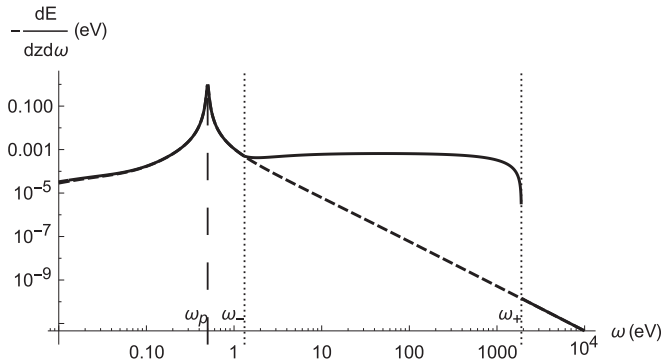

FIG. 2. Collisional energy loss spectrum of electron with $\gamma = 100$ in a semimetal with parameters $\omega_p = 0.5$ eV, $\Gamma = 0.025$ eV (so that its conductivity is 10 eV at room tempearture) [11] and $m = 0.5$ MeV. Solid line: $\sigma_\chi = 0.19$ eV [12,13], dashed line: $\sigma_\chi = 0$. $\omega_\pm$ are defined in (13). The seeming discontinuity at $\omega = \omega_+$ is a visual artifact.

and the identity

$$i\hat{\boldsymbol{k}} \times \boldsymbol{\epsilon}_{\lambda k} = \lambda \boldsymbol{\epsilon}_{\lambda k}. \quad (3)$$

Summations over λ are performed using the polarization sums given in Appendix in Ref. [9]. The space-time dependence of the electromagnetic field given by the integrals (2a) and (2b) was approximately evaluated in Refs. [9,15,16] assuming the low frequency limit of a conductor $\epsilon = 1 + i\sigma/\omega$ and used to compute the effect of the chiral anomaly on the magnetic field produced in relativistic heavy-ion collisions.

To compute the energy loss we need only the frequency components of the fields, see (10). These can be computed exactly. For illustration, consider

$$\boldsymbol{B}_\omega(\boldsymbol{r}) = \int \frac{d^2k_\perp}{(2\pi)^2} \frac{q k e^{i\omega z/v + i\boldsymbol{k}_\perp \cdot \boldsymbol{b}}}{[k_\perp^2 + \omega^2(1/v^2 - \epsilon)]^2 - (\sigma_\chi k)^2}$$
$$\times \left\{ [k_\perp^2 + \omega^2(1/v^2 - \epsilon)] \sum_\lambda \lambda \boldsymbol{\epsilon}_{\lambda k}(\hat{\boldsymbol{z}} \cdot \boldsymbol{\epsilon}_{\lambda\boldsymbol{k}}^*) \right.$$
$$\left. + \sigma_\chi k \sum_\lambda \boldsymbol{\epsilon}_{\lambda k}(\hat{\boldsymbol{z}} \cdot \boldsymbol{\epsilon}_{\lambda\boldsymbol{k}}^*) \right\}. \quad (4)$$

Its azimuthal component is

$$B_{\phi\omega}(\boldsymbol{r}) = \int \frac{d^2k_\perp}{(2\pi)^2} \frac{q k e^{i\omega z/v + i\boldsymbol{k}_\perp \cdot \boldsymbol{b}}}{[k_\perp^2 + \omega^2(1/v^2 - \epsilon)]^2 - (\sigma_\chi k)^2}$$
$$\times \left\{ [k_\perp^2 + \omega^2(1/v^2 - \epsilon)] \frac{-ik_\perp}{k} \cos\theta \right.$$
$$\left. + \sigma_\chi k \frac{-k_z k_\perp}{k^2} \sin\theta \right\}, \quad (5)$$

where $\boldsymbol{k}_\perp \cdot \boldsymbol{b} = k_\perp b \cos\theta$. Integration over θ and then over $k_\perp$ yields (6a) below. Other field components an be obtained in a similar way with the following result:

$$B_{\phi\omega}(\boldsymbol{r}) = \frac{q}{2\pi} \frac{e^{i\omega z/v}}{k_1^2 - k_2^2} \sum_{\nu=1}^2 (-1)^{\nu+1} k_\nu (k_\nu^2 - s^2) K_1(bk_\nu), \quad (6a)$$

$$B_{b\omega}(\boldsymbol{r}) = \sigma_\chi \frac{q}{2\pi} \frac{i\omega}{v} \frac{e^{i\omega z/v}}{k_1^2 - k_2^2} \sum_{\nu=1}^2 (-1)^\nu k_\nu K_1(bk_\nu), \quad (6b)$$

$$B_{z\omega}(\boldsymbol{r}) = \sigma_\chi \frac{q}{2\pi} \frac{e^{i\omega z/v}}{k_1^2 - k_2^2} \sum_{\nu=1}^2 (-1)^{\nu+1} k_\nu^2 K_0(bk_\nu), \quad (6c)$$

$$E_{z\omega}(\boldsymbol{r}) = \frac{q}{2\pi} \frac{i\omega}{v^2\epsilon} \frac{e^{i\omega z/v}}{k_1^2 - k_2^2} \sum_{\nu=1}^2 (-1)^{\nu+1}$$
$$\times [(v^2\epsilon - 1)(k_\nu^2 - s^2) - \sigma_\chi^2] K_0(bk_\nu), \quad (6d)$$

$$E_{b\omega}(\boldsymbol{r}) = \frac{q}{2\pi} \frac{1}{v\epsilon} \frac{e^{i\omega z/v}}{k_1^2 - k_2^2} \sum_{\nu=1}^2 (-1)^{\nu+1} k_\nu$$
$$\times (k_\nu^2 - s^2 - \sigma_\chi^2) K_1(bk_\nu), \quad (6e)$$

$$E_{\phi\omega}(\boldsymbol{r}) = v B_{b\omega}(\boldsymbol{r}), \quad (6f)$$

where

$$k_\nu^2 = s^2 - \frac{\sigma_\chi^2}{2} + (-1)^\nu \sigma_\chi \sqrt{\omega^2 \epsilon + \frac{\sigma_\chi^2}{4}} \qquad (7)$$

with $\nu = 1, 2$ and

$$s^2 = \omega^2 \left[\frac{1}{v^2} - \epsilon(\omega) \right]. \qquad (8)$$

Without loss of generality we assume that $\sigma_\chi > 0$ which implies that $k_2^2 > k_1^2$. The plasma permittivity is well described by

$$\epsilon = 1 - \frac{\omega_p^2}{\omega^2 + i\omega\Gamma}, \qquad (9)$$

where ω_p is the plasma frequency and the damping constant Γ is related to the electrical conductivity.

III. COLLISIONAL ENERGY LOSS

The energy loss rate can be computed as the flux of the Poynting vector out of a cylinder of radius a coaxial with the particle path. For a particle moving with velocity v along the z-axis the total loss per unit length reads

$$-\frac{d\varepsilon}{dz} = 2\pi a \int_{-\infty}^{\infty} (E_\phi B_z - E_z B_\phi) dt$$

$$= 2a \operatorname{Re} \int_0^{\infty} (E_{\phi\omega} B_{z\omega}^* - E_{z\omega} B_{\phi\omega}^*) d\omega. \qquad (10)$$

To calculate the integral over ω we first isolate the contribution of the pole in $1/\epsilon$ at $\omega = \omega_p$ using the rule

$$\frac{1}{\epsilon} = \frac{\omega^2}{\omega^2 - \omega_p^2 + i0} = -i\pi\omega_p^2 \delta(\omega^2 - \omega_p^2) + \mathcal{P}\frac{\omega^2}{\omega^2 - \omega_p^2}, \qquad (11)$$

where it is assumed that $\Gamma \ll \omega_p$. Substituting the field components from (6) into (10) and replacing $1/\epsilon$ by its imaginary part one derives

$$-\frac{d\varepsilon^{\text{pole}}}{dz} = \frac{q^2 \omega_p^2}{4\pi v^2} K_0(a\omega_p/v) \operatorname{Re}\left\{ a\sqrt{\omega_p^2/v^2 - \sigma_\chi^2} K_1\left(a\sqrt{\omega_p^2/v^2 - \sigma_\chi^2}\right) \right\}. \qquad (12)$$

Away from the pole, the permittivity is real. In this case the contribution to the integral over ω comes from those domains of ω where at least one of k_ν's is imaginary. There are two such domains (A) and (B). In domain (A) $k_1^2 < k_2^2 < 0$. Inspection of (7) reveals that $k_2^2 < 0$ if either $\omega^2 > \omega_+^2$ or $\omega^2 < \omega_-^2$ where

$$\omega_\pm^2 = \frac{-2(1/v^2 - 1)\omega_p^2 + \sigma_\chi^2/v^2 \pm \sqrt{\left[2(1/v^2 - 1)\omega_p^2 - \sigma_\chi^2/v^2\right]^2 - 4(1/v^2 - 1)^2\omega_p^4}}{2(1/v^2 - 1)^2}. \qquad (13)$$

Additionally, if $\omega_p < \sigma_\chi/\sqrt{2}$ the inequality

$$0 < \omega < \sqrt{\frac{\sigma_\chi^2/2 - \omega_p^2}{1/v^2 - 1}} \qquad (14)$$

must be satisfied. Domain (B), $k_1^2 < 0 < k_2^2$, corresponds to in the interval $\omega_-^2 < \omega^2 < \omega_+^2$. We note that in vacuum,[1] i.e. when $\omega_p = 0$ domain (A) is empty because (13) and (14) are never satisfied at any σ_χ. In contrast, when $\sigma_\chi = 0$, domain (B) is empty because then $k_1 = k_2$.

It can be readily verified that $\operatorname{Im} k_1 < 0$ at all ω's, while $\operatorname{Im} k_2 < 0$ when $\epsilon > 0$ and positive otherwise. It is not difficult to compute the real part of the Poynting vector in both cases. However, later we will be primarily concerned with the ultrarelativistic limit $v \to 1$ in which the energy loss is dominated by high frequencies $\omega \gg \omega_p$. In this case $\epsilon > 0$ and the imaginary parts of $k_{1,2}$ are negative. It is convenient to denote $k_+^2 = -k_1^2$ and $k_-^2 = -k_2^2$, so that in domain (A) $\operatorname{Im} k_{1,2} = k_\pm < 0$ while in domain (B) $\operatorname{Im} k_1 = k_+ < 0$. We derive

$$\operatorname{Re}(E_{\phi\omega} B_{z\omega}^*)|_{(A)} = \frac{q^2}{(2\pi)^2} \frac{\sigma_\chi^2 \omega}{(k_+^2 - k_-^2)^2} \left\{ \frac{\pi}{2a}(k_+^2 + k_-^2) - \frac{\pi^2}{4} k_+ k_-^2 [J_1(ak_+)Y_0(ak_-) - J_0(ak_-)Y_1(ak_+)] \right.$$

$$\left. - \frac{\pi^2}{4} k_+^2 k_- [J_1(ak_-)Y_0(ak_+) - J_0(ak_+)Y_1(ak_-)] \right\}, \qquad (15)$$

$$\operatorname{Re}(E_{\phi\omega} B_{z\omega}^*)|_{(B)} = \frac{q^2}{(2\pi)^2} \frac{\sigma_\chi^2 \omega}{(k_+^2 - k_-^2)^2} \left\{ \frac{\pi}{2a} k_+^2 - \frac{\pi}{2} k_2^2 k_+ J_1(ak_+)K_0(ak_2) + \frac{\pi}{2} k_+^2 k_2 K_1(ak_2)J_0(ak_+) \right\}, \qquad (16)$$

$$\operatorname{Re}(E_{z\omega} B_{\phi\omega}^*)|_{(A)} = \frac{q^2}{(2\pi)^2} \frac{\omega}{v^2 \epsilon (k_+^2 - k_-^2)^2} \left\{ -\frac{\pi}{2a}[(v^2\epsilon - 1)(k_+^2 + s^2) + \sigma_\chi^2](k_+^2 + s^2) - \frac{\pi}{2a}[(v^2\epsilon - 1)(k_-^2 + s^2) + \sigma_\chi^2] \right.$$

[1] The term "vacuum" refers to Eqs. (1) with $\epsilon = 1$ and finite σ_χ, which is a version of axion electrodynamics [17]

$$\times (k_-^2 + s^2) - \frac{\pi^2}{4} \big[(v^2\epsilon - 1)(k_+^2 + s^2) + \sigma_\chi^2\big](k_-^2 + s^2)k_-[J_0(ak_+)Y_1(ak_-) - J_1(ak_-)Y_0(ak_+)]$$

$$-\frac{\pi^2}{4}\big[(v^2\epsilon - 1)(k_-^2 + s^2) + \sigma_\chi^2\big](k_+^2 + s^2)k_+[J_0(ak_-)Y_1(ak_+) - J_1(ak_+)Y_0(ak_-)]\bigg\}, \tag{17}$$

$$\mathrm{Re}\,(E_{z\omega}B_{\phi\omega}^*)|_{(B)} = \frac{q^2}{(2\pi)^2}\frac{\omega}{v^2\epsilon(k_+^2 - k_-^2)^2}\bigg\{-\frac{\pi}{2a}\big[(v^2\epsilon - 1)(k_+^2 + s^2) + \sigma_\chi^2\big](k_+^2 + s^2)$$

$$-\frac{\pi}{2}\big[(v^2\epsilon - 1)(k_+^2 + s^2) + \sigma_\chi^2\big](s^2 - k_2^2)k_2 J_0(ak_+)K_1(ak_2)$$

$$-\frac{\pi}{2}\big[(v^2\epsilon - 1)(s^2 - k_2^2) + \sigma_\chi^2\big](k_+^2 + s^2)k_+ J_1(ak_+)K_0(ak_2)\bigg\}. \tag{18}$$

Substituting these equations into (10) we obtain frequency spectrum of the energy loss $-d\varepsilon/dzd\omega$ which is plotted in Figs. 1 and 2. The ω integral can be computed exactly in several important approximations that we now consider.

A. Ultrarelativistic limit

In the limit $ak_\nu \ll 1$, the contribution of the pole (12) is proportional to large logarithm $\ln a$, the term (18) is independent of a, whereas the remaining terms are suppressed by the positive powers of ak_ν. The corresponding energy loss reads

$$-\frac{d\varepsilon}{dz} = \frac{q^2}{4\pi}\frac{\omega_p^2}{v^2}\ln\frac{1.12v}{a\omega_p}$$

$$-\frac{q^2}{4\pi}\int_{k_1^2<0<k_2^2}\frac{\omega}{v^2\epsilon}\frac{(s^2 - k_1^2)(v^2\epsilon - 1) + \sigma_\chi^2}{k_1^2 - k_2^2}d\omega. \tag{19}$$

The integration domain (B) simplifies in the ultrarelativistic limit $v \to 1$: $\omega_p^2/\sigma_\chi < \omega < \gamma^2\sigma_\chi$, where $\gamma = (1 - v^2)^{-1/2}$. Expanding the integrand at large frequencies, assuming $\omega \gg \sigma_\chi$, yields

$$-\frac{q^2}{4\pi}\frac{1}{2\sigma_\chi}\int^{\gamma^2\sigma_\chi}\bigg(-\frac{\sigma_\chi\omega}{\gamma^2} + \sigma_\chi^2\bigg)d\omega, \tag{20}$$

where the precise value of the lower limit is irrelevant as long as $\gamma \gg 1$. Integrating one obtains

$$-\frac{d\varepsilon}{dz} = \frac{q^2}{4\pi v^2}\bigg(\omega_p^2\ln\frac{v}{a\omega_p} + \frac{1}{4}\gamma^2\sigma_\chi^2\bigg). \tag{21}$$

We observe that the energy loss due to the anomaly, represented by the second term in (21), dominates at high energies. Inclusion of quantum effects produces the logarithmic dependence of the first term on γ but this does not change our conclusion.

B. Nonchiral medium

In the limit $\sigma_\chi \to 0$ the contributions of (15), (16), and (18) vanish. The finite limit emerges from (17) which along with (12) yields

$$-\frac{d\varepsilon}{dz} = \frac{q^2}{4\pi}\frac{\omega_p^2}{v^2}K_0(a\omega_p/v)(a\omega_p/v)K_1(a\omega_p/v)$$

$$+\frac{q^2}{4\pi v^2}\int_{s^2<0}\omega\bigg(v^2 - \frac{1}{\epsilon}\bigg)d\omega. \tag{22}$$

The second term vanishes in plasma since $\epsilon < 1$ implies that s^2 is always positive, see (8) and (9). However, if medium contains bound states, then the second term contributes when the velocity of the particle is larger than the phase velocity of light in the medium. A single bound state of frequency ω_0 contributes to the permittivity as

$$\epsilon(\omega) = 1 - \frac{\omega_p^2}{\omega^2 - \omega_0^2 + i\omega\Gamma} \tag{23}$$

In this case (22) is generalized as

$$-\frac{d\varepsilon}{dz} = \frac{q^2}{4\pi}\frac{\omega_p^2}{v^2}K_0\big(a\sqrt{\omega_p^2 + \omega_0^2}/v\big)\big(a\sqrt{\omega_p^2 + \omega_0^2}/v\big)$$

$$\times K_1\big(a\sqrt{\omega_p^2 + \omega_0^2}/v\big) + \frac{q^2}{4\pi v^2}\int_{s^2<0}\omega\bigg(v^2 - \frac{1}{\epsilon}\bigg)d\omega. \tag{24}$$

Neglecting Γ, the integration region $s^2 < 0$ is equivalent to $(1 - \epsilon(0)v^2)/(1 - v^2) < \omega^2/\omega_0^2 < 1$ if $v < 1/\sqrt{\epsilon(0)}$ and to $\omega < \omega_0$ if $v > 1/\sqrt{\epsilon(0)}$. Integration over ω in the second term yields the well-known Fermi's result [8].

C. Cherenkov radiation

Some of the collisional energy loss emerges in the form of the Cherenkov radiation. In the nonchiral medium it is included in the second term in (22) (provided that $\epsilon(0)$ is finite, as explained in the previous subsection) and is small compared to the large first term that describes excitation of the longitudinal oscillations in the medium (medium polarization).

In the chiral medium the Cherenkov radiation emerges even when $\epsilon = 1$, which is known as the chiral (or, in a different context, vacuum) Cherenkov radiation [18–21].[2] It is generated by the anomalous electromagnetic current in the presence of the moving charged particle. The Cherenkov radiation is that part of the total energy flux moving radially away from the particle which is finite at $a \to \infty$. It can be computed by replacing the Bessel functions appearing in (15)–(18) with their asymptotic expressions. In particular, the

---

[2]It was proposed to be a test of the Lorentz symmetry violation in Refs. [17–19,22–28].

rate of the chiral Cherenkov radiation emitted in a unit interval of frequencies by an ultrarelativistic particle in empty space ($\epsilon = 1$) is given by

$$\frac{dW}{d\omega} = -\frac{d\varepsilon}{dz\omega d\omega}\bigg|_{a\to\infty}$$
$$= \frac{q^2}{4\pi}\left\{\frac{1}{2}\left(1 - \frac{1}{v^2}\right) + \frac{\sigma_\chi}{2\omega} + \frac{(1+v^2)\sigma_\chi^2}{8v^2\omega^2} + \cdots\right\},$$
$$\omega < \sigma_\chi\gamma^2. \tag{25}$$

which comes about from (18). Expansion in powers of σ_χ/ω is justified for the ultrarelativistic particle. Equation (25) is derived neglecting the fermion recoil which proportional to $\hbar\omega$. It is a good approximation as long as $\omega_+ = \sigma_\chi\gamma^2 \ll \varepsilon$, in other words when $\gamma \ll m/\sigma_\chi$, where m is the particle mass. The total radiated power P is obtained by integrating (25) over $\omega d\omega$. It is dominated by the upper limit so that only the first two terms contribute at large γ with the result:

$$P = \frac{q^2}{4\pi}\frac{\sigma_\chi^2\gamma^2}{4}. \tag{26}$$

We observe that the spectrum (25) is exactly the same as (20) which indicates that all energy lost by the ultrarelativistic particle due to the anomalous current is radiated as the chiral Cherenkov radiation.

The spectrum of the chiral Cherenkov radiation was previously computed by one of the authors in the leading order of QED with the result [20]

$$\frac{dW^{\text{quant}}}{d\omega} = \frac{q^2}{(4\pi)2\omega}\left\{\sigma_\chi\left(\frac{x^2}{2} - x + 1\right) - \frac{m^2}{\varepsilon}x\right\}, \quad \omega < \omega_M, \tag{27}$$

where $x = \omega/\varepsilon$ is the fraction of the fermion energy carried away by the radiated photon and

$$\omega_M = \frac{\varepsilon}{1 + m^2/(\sigma_\chi\varepsilon)}. \tag{28}$$

Photon spectrum always extends all the way to ω_M since $\omega_M < \sigma_\chi\gamma^2$. Moreover, since $\omega_M < \varepsilon$ and hence $x < 1$, (27) is valid even at $\gamma \gg m/\sigma_\chi$, in contrast to the classical formula (25). The classical limit of (27) is recovered in the limit $x \ll 1$: the term in (27) proportional to σ_χ reduces to the second term in (25), while the second term in (27) reduces to the first term in (25). The total radiation power is

$$P^{\text{quant}} = \frac{q^2}{4\pi}\frac{\sigma_\chi\varepsilon}{3}, \tag{29}$$

where the terms of order $m/\varepsilon = 1/\gamma$ were neglected. Evidently, the effect of the recoil on the energy loss is to reduce the energy dependence from ε^2 to ε.

IV. DISCUSSION

The classical calculation performed in this paper captures the main feature of the energy loss in chiral medium, namely, its much faster increase with the particle energy that in a nonchiral medium. Taking the recoil effects into account, the energy loss is proportional to energy ε. In contrast, energy dependence of the collisional energy loss in nonchiral medium

is at most logarithmic. The conventional radiative energy loss is likewise proportional to energy in the noncoherent Bethe-Heitler (BH) regime. The ratio of the energy loss due to the chiral Cherenkov (χC) effect to the conventional radiative loss is

$$\frac{\Delta\varepsilon^{\chi C}}{\Delta\varepsilon^{\text{BH}}} \sim \frac{\sigma_\chi}{e^2T} \sim \frac{\mu_5}{T}, \tag{30}$$

where T is the plasma temperature and μ_5 is the axial chemical potential. The coherence effects reduce the energy dependence of the radiative energy loss to $\sqrt{\varepsilon}$ (see review [29]). This significantly increases the ratio (30). In this paper we assumed that distribution of the topological charge density is homogenous and therefore there are no coherence effects on the chiral Cherenkov radiation. This is a good approximation as long as the coherence length associated with photon radiation is smaller than the distance over which the topological charge density significantly varies. This maybe the case in the nuclear matter where there is evidence—supported by the theoretical arguments [30,31]—of the topological domains of nearly constant density in wide range of temperatures [32–39].

Figure 1 displays the spectrum of the collisional energy loss by a fast particle in quark-gluon plasma computed using the results of Sec. III. We emphasize that this is a purely electromagnetic effect. The chiral Cherenkov radiation emerges as a bump between ω_- and ω_+. The relevant parameters are inferred from the lattice calculations [10] or by the way of educated guess in the case of the chiral conductivity. The quantum corrections due to the recoil would shift the UV endpoint of the anomalous contribution to the left since $\omega_M < \omega_+ = \sigma_\chi\gamma^2$. However, the overall effect of the recoil is not that significant since $\omega_M = 0.44\varepsilon$ is not too close to unity. The rate of energy loss due to the anomaly is about $\dot{\varepsilon}/\varepsilon \sim 10^{-4}$ per unit fm regardless of particle energy as indicated by (29).

Hitherto we have discussed the electromagnetic part of the collisional energy loss. Our results can be readily generalized to the strong interactions which dominate the particle energy loss in QGP [40]. Thus, marking the quantities computed in QCD by a tilde sign, (21) becomes:

$$-\frac{d\varepsilon}{dz} = \frac{g^2C_F}{4\pi v^2}\left(\frac{\tilde{\omega}_p^2}{2N_c^2}\ln\frac{v}{a\tilde{\omega}_p} + \frac{1}{4}\gamma^2\tilde{\sigma}_\chi^2\right), \tag{31}$$

where g is the strong coupling. The plasma frequency $\tilde{\omega}_p$ is obtained from ω_p by replacing $e \to \sqrt{N_c}g$ [41]. In (21) the chiral conductivity σ_χ is proportional to the QED anomaly coefficient $c_A = (N_c/3)(e^2/16\pi^2)$ while $\tilde{\sigma}_\chi$ is proportional to the QCD anomaly coefficient $\tilde{c}_A = N_f g^2/16\pi^2$. The energy loss due to the chiral anomaly is given by the second term in (31). With the account of the recoil the anomalous contribution becomes

$$-\frac{d\varepsilon}{dz}\bigg|_{\text{anom}} = \frac{g^2C_F}{4\pi}\frac{\tilde{\sigma}_\chi\varepsilon}{3}, \tag{32}$$

which is the QCD version of (29). Accordingly, the rate of energy loss due to the chiral anomaly of QCD is about $(\alpha_s/\alpha_{\text{em}})^2$ which makes it 10^3–10^4 times larger in QCD than in QED. In view of our estimates in the previous paragraph, the chiral anomaly of QCD may induce the rate of energy loss up to $\dot{\varepsilon}/\varepsilon \sim 1$ per fm, meaning that the particle energy

decreases by a factor of three over each fm it travels regardless of its initial energy. Moreover, the coherence effects slow down the increase with energy of the conventional energy loss mechanisms which brings about the increase with energy of the relative contribution of the chiral Cherenkov radiation. Clearly, a numerical evaluation of the chiral conductivity would be of considerable benefit to the QGP phenomenology.

In an anisotropic chiral medium such as Weyl semimetals there is an additional anomalous current $\boldsymbol{j}_{AH} = \boldsymbol{b} \times \boldsymbol{E}$ that generates the anomalous Hall effect [22,42,43]. Parameter $\boldsymbol{b}$ is the distance between the Weyl nodes in the momentum space (not to be confused with the impact parameter used in Sec. II). The spectrum of the corresponding chiral Cherenkov radiation was computed in Ref. [44]. In the ultrarelativistic limit, the energy loss equals the total radiated power and is given by (29) with σ_χ replaced by b (assuming that electron's velocity is parallel to $\boldsymbol{b}$). To estimate the energy loss in a semimetal reported in Refs. [12,13] we use $b = (\alpha/\pi)80$ eV. According to (30) at room temperatures most of energy is lost

due to chiral Cherenkov radiation. The energy loss spectrum for a typical semimetal computed using the results of Sec. III is displayed in Fig. 2. The recoil effect is negligible since $\omega_M \lesssim \sigma_\chi \gamma^2 \ll \varepsilon$. One observes significant enhancement of the ultraviolet and x-ray regions of the photon spectrum which presents an exciting opportunity for experimental study of the chiral anomaly effects.

In this paper we computed the leading order contribution to the collisional energy loss due to the chiral anomaly. It turned out to be significant, motivating us to investigate the higher order contributions. If the theory of the conventional energy loss (see, e.g., Ref. [29]) is a guide, we anticipate that those contributions will substantially modify the leading order result.

[1] K. Fukushima, D. E. Kharzeev, and H. J. Warringa, The chiral magnetic effect, Phys. Rev. D **78**, 074033 (2008).

[2] D. Kharzeev, Parity violation in hot QCD: Why it can happen, and how to look for it, Phys. Lett. B **633**, 260 (2006).

[3] D. E. Kharzeev, L. D. McLerran, and H. J. Warringa, The effects of topological charge change in heavy ion collisions: 'Event by event P and CP violation', Nucl. Phys. A **803**, 227 (2008).

[4] D. E. Kharzeev, Topologically induced local P and CP violation in QCD × QED, Ann. Phys. **325**, 205 (2010).

[5] D. Kharzeev and A. Zhitnitsky, Charge separation induced by P-odd bubbles in QCD matter, Nucl. Phys. A **797**, 67 (2007).

[6] S. L. Adler, Axial vector vertex in spinor electrodynamics, Phys. Rev. **177**, 2426 (1969).

[7] J. S. Bell and R. Jackiw, A PCAC puzzle: $\pi_0 \rightarrow \gamma\gamma$ in the sigma model, Nuovo Cim. A **60**, 47 (1969).

[8] E. Fermi, The ionization loss of energy in gases and in condensed materials, Phys. Rev. **57**, 485 (1940).

[9] K. Tuchin, Electromagnetic field of ultrarelativistic charge in topologically random nuclear matter, Nucl. Phys. A **1001**, 121907 (2020).

[10] H. T. Ding, A. Francis, O. Kaczmarek, F. Karsch, E. Laermann, and W. Soeldner, Thermal dilepton rate and electrical conductivity: An analysis of vector current correlation functions in quenched lattice QCD, Phys. Rev. D **83**, 034504 (2011).

[11] X. Huang, L. Zhao, Y. Long, P. Wang, D. Chen, Z. Yang, H. Liang, M. Xue, H. Weng, Z. Fang *et al.*, Observation of the Chiral-Anomaly-Induced Negative Magnetoresistance in 3D Weyl Semimetal TaAs, Phys. Rev. X **5**, 031023 (2015).

[12] B. Q. Lv *et al.*, Experimental discovery of Weyl semimetal TaAs, Phys. Rev. X **5**, 031013 (2015).

[13] S. Y. Xu *et al.*, Discovery of a Weyl Fermion semimetal and topological Fermi arcs, Science **349**, 613 (2015).

[14] D. E. Kharzeev and H. J. Warringa, Chiral magnetic conductivity, Phys. Rev. D **80**, 034028 (2009).

[15] K. Tuchin, Electromagnetic field and the chiral magnetic effect in the quark-gluon plasma, Phys. Rev. C **91**, 064902 (2015).

[16] H. Li, X. l. Sheng, and Q. Wang, Electromagnetic fields with electric and chiral magnetic conductivities in heavy ion collisions, Phys. Rev. C **94**, 044903 (2016).

[17] S. M. Carroll, G. B. Field, and R. Jackiw, Limits on a Lorentz and parity violating modification of electrodynamics, Phys. Rev. D **41**, 1231 (1990).

[18] R. Lehnert and R. Potting, Vacuum Cherenkov Radiation, Phys. Rev. Lett. **93**, 110402 (2004).

[19] R. Lehnert and R. Potting, The Cerenkov effect in Lorentz-violating vacua, Phys. Rev. D **70**, 125010 (2004); **70**, 129906(E) (2004).

[20] K. Tuchin, Radiative instability of quantum electrodynamics in chiral matter, Phys. Lett. B **786**, 249 (2018).

[21] X. G. Huang and K. Tuchin, Transition Radiation as a Probe of the Chiral Anomaly, Phys. Rev. Lett. **121**, 182301 (2018).

[22] F. R. Klinkhamer and G. E. Volovik, Emergent CPT violation from the splitting of Fermi points, Int. J. Mod. Phys. A **20**, 2795 (2005).

[23] V. A. Kostelecky and A. G. M. Pickering, Vacuum Photon Splitting In Lorentz Violating Quantum Electrodynamics, Phys. Rev. Lett. **91**, 031801 (2003).

[24] D. Mattingly, Modern tests of Lorentz invariance, Living Rev. Rel. **8**, 5 (2005).

[25] T. Jacobson, S. Liberati, and D. Mattingly, Lorentz violation at high energy: Concepts, phenomena and astrophysical constraints, Ann. Phys. **321**, 150 (2006).

[26] B. Altschul, Vacuum Cerenkov Radiation in Lorentz-Violating Theories without CPT Violation, Phys. Rev. Lett. **98**, 041603 (2007).

[27] B. Altschul, Cerenkov radiation in a Lorentz-violating and birefringent vacuum, Phys. Rev. D **75**, 105003 (2007).

[28] J. R. Nascimento, E. Passos, A. Y. Petrov, and F. A. Brito, Lorentz-CPT violation, radiative corrections and finite temperature, J. High Energy Phys. 06 (2007) 016.

[29] S. Peigné and A. V. Smilga, Energy losses in a hot plasma revisited, Phys. Usp. **52**, 659 (2009).

[30] A. R. Zhitnitsky, P odd fluctuations and long range order in heavy ion collisions: Deformed QCD as a toy model, Nucl. Phys. A **897**, 93 (2013).

[31] A. R. Zhitnitsky, QCD as a topologically ordered system, Ann. Phys. **336**, 462 (2013).

[32] I. Horvath, S. J. Dong, T. Draper, F. X. Lee, K. F. Liu, N. Mathur, H. B. Thacker, and J. B. Zhang, Low dimensional long range topological charge structure in the QCD vacuum, Phys. Rev. D **68**, 114505 (2003).

[33] I. Horvath, A. Alexandru, J. B. Zhang, Y. Chen, S. J. Dong, T. Draper, F. X. Lee, K. F. Liu, N. Mathur, S. Tamhankar, and H. B. Thacker, Inherently global nature of topological charge fluctuations in QCD, Phys. Lett. B **612**, 21 (2005).

[34] I. Horvath, A. Alexandru, J. B. Zhang, Y. Chen, S. J. Dong, T. Draper, K. F. Liu, N. Mathur, S. Tamhankar, and H. B. Thacker, The negativity of the overlap-based topological charge density correlator in pure-glue QCD and the non-integrable nature of its contact part, Phys. Lett. B **617**, 49 (2005).

[35] A. Alexandru, I. Horvath, and J. B. Zhang, The Reality of the fundamental topological structure in the QCD vacuum, Phys. Rev. D **72**, 034506 (2005).

[36] E. M. Ilgenfritz, K. Koller, Y. Koma, G. Schierholz, T. Streuer, and V. Weinberg, Exploring the structure of the quenched QCD vacuum with overlap fermions, Phys. Rev. D **76**, 034506 (2007).

[37] E. M. Ilgenfritz, D. Leinweber, P. Moran, K. Koller, G. Schierholz, and V. Weinberg, Vacuum structure revealed by over-improved stout-link smearing compared with the overlap analysis for quenched QCD, Phys. Rev. D **77**, 074502 (2008).

[38] A. V. Kovalenko, M. I. Polikarpov, S. N. Syritsyn, and V. I. Zakharov, Three dimensional vacuum domains in four dimensional SU(2) gluodynamics, Phys. Lett. B **613**, 52 (2005).

[39] F. Bruckmann, F. Gruber, N. Cundy, A. Schafer, and T. Lippert, Topology of dynamical lattice configurations including results from dynamical overlap fermions, Phys. Lett. B **707**, 278 (2012).

[40] D. d'Enterria, Jet quenching, Landolt-Bornstein **23**, 471 (2010).

[41] J. I. Kapusta and C. Gale, Finite-temperature field theory: Principles and applications (Cambridge University Press, 2006).

[42] A. A. Zyuzin and A. A. Burkov, Topological response in Weyl semimetals and the chiral anomaly, Phys. Rev. B **86**, 115133 (2012).

[43] A. G. Grushin, Consequences of a condensed matter realization of Lorentz violating QED in Weyl semi-metals, Phys. Rev. D **86**, 045001 (2012).

[44] K. Tuchin, Chiral Cherenkov and chiral transition radiation in anisotropic matter, Phys. Rev. D **98**, 114026 (2018).